JCIM JOURNAL OF CHEMICAL INFORMATION AND MODELING

Cite This: J. Chem. Inf. Model. 2018, 58, 2085−2091

Article

pubs.acs.org/jcim

Anion-π Interactions in Computer-Aided Drug Design: Modeling the Inhibition of Malate Synthase by Phenyl-Diketo Acids

Jill F. Ellenbarger,[‡,†] Inna V. Krieger,[§] Hsiao-ling Huang,[‡,§] Silvia Gómez-Coca,[‡,#] Thomas R. Ioerger,[∥] James C. Sacchettini,[‡,§] Steven E. Wheeler,[‡,▽] and Kim R. Dunbar*[,‡]

[‡]Department of Chemistry, Texas A&M University, P.O. Box 30012, College Station, Texas 77842, United States

[†]Department of Chemistry, John Brown University, 2000 West University Street, Siloam Springs, Arkansas 72761, United States

[§]Department of Biochemistry and Biophysics, Texas A&M University, 3112 TAMU, College Station, Texas 77842, United States

[#]Department of Chemistry, King's College London, 7 Trinity Street, London SE1 1DB, U.K.

[∥]Department of Computer Science and Engineering, Texas A&M University, 3112 TAMU, College Station, Texas 77842, United States

[▽]Center for Computational Quantum Chemistry, Department of Chemistry, University of Georgia, 140 Cedar Street, Athens, Georgia 30602-2556, United States

Supporting Information

ABSTRACT: Human infection by *Mycobacterium tuberculosis* (Mtb) continues to be a global epidemic. Computer-aided drug design (CADD) methods are used to accelerate traditional drug discovery efforts. One noncovalent interaction that is being increasingly identified in biological systems but is neglected in CADD is the anion-π interaction. The study reported herein supports the conclusion that anion-π interactions play a central role in directing the binding of phenyl-diketo acid (PDKA) inhibitors to malate synthase (GlcB), an enzyme required for *Mycobacterium tuberculosis* virulence. Using density functional theory methods (M06-2X/6-31+G(d)), a GlcB active site template was developed for a predictive model through a comparative analysis of PDKA-bound GlcB crystal structures. The active site model includes the PDKA molecule and the protein determinants of the electrostatic, hydrogen-bonding, and anion-π interactions involved in binding. The predictive model accurately determines the Asp 633-PDKA structural position upon binding and precisely predicts the relative binding enthalpies of a series of 2-ortho halide-PDKAs to GlcB. A screening model was also developed to efficiently assess the propensity of each PDKA analog to participate in an anion-π interaction; this method is in good agreement with both the predictive model and the experimental binding enthalpies for the 2-ortho halide-PDKAs. With the screening and predictive models in hand, we have developed an efficient method for computationally screening and evaluating the binding enthalpy of variously substituted PDKA molecules. This study serves to illustrate the contribution of this overlooked interaction to binding affinity and demonstrates the importance of integrating anion-π interactions into structure-based CADD.

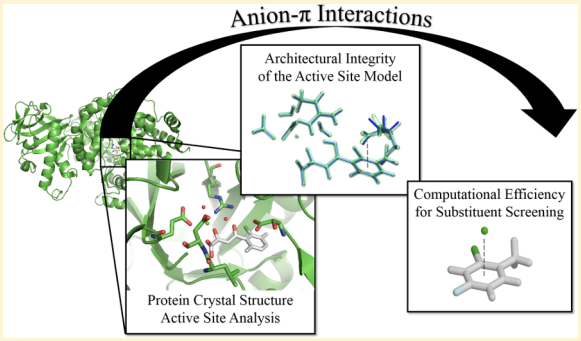

INTRODUCTION

Tuberculosis (TB) was responsible for over 1.3 million deaths and an additional 10.4 million new incidents of infection in 2016 alone.[1] While TB cases are often successfully treated with first- and second-line drugs, this disease continues to threaten the global population due to ever-increasing drug resistance and indefinite persistence of *Mycobacterium tuberculosis* (*Mtb*), the pathogen responsible for TB infection.[1−3]

In response to the continued threat of drug-resistant bacteria such as *Mtb*, it is imperative that researchers use an arsenal of modern techniques in the pursuit of new drugs. In this vein, computer aided drug development (CADD) methodologies are extremely useful when applied in tandem with traditional drug discovery methods to efficiently identify efficacious drug molecules through structure-based and ligand-based methods.[4,5] Structure-based methods screen the environment of the target protein's active site against a library of potential binders.[4] Such exhaustive efforts are important for identifying classes of promising molecular scaffolds that are more likely to exhibit appreciable binding and efficacy. Current algorithms typically consider steric, electrostatic, hydrophobic/hydrophilic, and hydrogen-bonding contributions to binding, but these algorithms do not properly account for the interplay of weak, noncovalent interactions that involve aromatic π systems.[4] Yet, in many biological systems, subtle interactions involving aromatic π systems have been shown to greatly influence the binding affinity and selectivity of substrates.[6,7]

Received: June 25, 2018
Published: August 23, 2018

DOI: 10.1021/acs.jcim.8b00417
J. Chem. Inf. Model. 2018, 58, 2085−2091

Therefore, more sophisticated, higher-level computational methods are required to take into account these noncovalent interactions.

This study presents the development of a structure-based computational approach to modeling the inhibition of malate synthase (GlcB), an enzyme involved in the glyoxylate shunt of the tricarboxylic acid (TCA) cycle of *Mtb*.[8−11] GlcB facilitates the reaction between glyoxlyate and acetyl-coenzyme A to form malate, and this protein is necessary for the virulence and persistence of *Mtb*.[12,13] Additionally, GlcB has been targeted for drug development because it has a large, accessible active site and has no homologue in humans.[13−15] Sacchettini and co-workers screened a series of molecules with glyoxylate-like moieties for GlcB inhibition and found that a phenyl-diketo acid (PDKA) had activity. This hit was developed into a series of PDKAs with various substituents around the aromatic ring (Figure 1a), and the PDKA series demonstrated a favorable combination of inhibition, whole cell potency, and low toxicity.[10] Protein crystallography studies identified that the PDKA inhibitors coordinate to the catalytic magnesium ion in GlcB, occupy the active site pocket, and interact with the nearby residues through a series of noncovalent interactions, including an anion-π contact (Figure 1b).[10] The carboxylate portion of the Asp residue generally packs face-on to the π-cloud of the aromatic ring, and the mean contact distance is ~3.5 Å (less than the typical ~4.5 Å distance of hydrophobic contacts,[16] suggesting an anion-π interaction). Furthermore, adding substituents around the ring differentially affected the affinity of the compound, supporting the importance of the anion-π interaction in the PDKA inhibition of GlcB.

Anion-π interactions are broadly defined as attractive, noncovalent interactions between an anion and an aromatic system and are being increasingly identified in biological systems.[7,16−21] These weak contacts can be described as attractive substituent-driven, ion-dipole interactions and contrast with cation-π interactions, which are driven by the electrostatic interaction between the positive charge of the ion and the negative charge of the π-cloud.[6,22,23]

The study of the noncovalent interactions, particularly the anion-π interaction, involved in PDKA binding to GlcB has generated interest in designing PDKAs that leverage such intermolecular interactions to increase inhibition activity. After the testing of a limited set of PDKAs with singly substituted aromatic rings, it became apparent that both the nature and the combination of the substituents influence the IC_{50} values (Table 1). Most importantly, from the perspective of the present study, is the fact that these data could not be explained in terms of conventional noncovalent interactions nor Hammett-like equations involving substituent electronegativity and that these data likely stem from the influence of the substituents on the anion-π interaction between the Asp 633 residue of GlcB and the aromatic ring of the inhibitor. The identification of optimal PDKA molecules using current predictive methods was impeded because standard computational approaches (i.e., ligand docking, molecular dynamics, pharmacophore modeling, etc.) did not appropriately or efficiently account for the critical anion-π interactions.[4]

Frontera and co-workers created an active site model from the PDKA-bound GlcB crystal structures to explore anion-π and long-range electrostatic interactions using computational *ab initio* methods.[24] The results of full, unconstrained geometry optimizations of these model active sites led the authors to predict an increase in binding efficacy for the per-F-

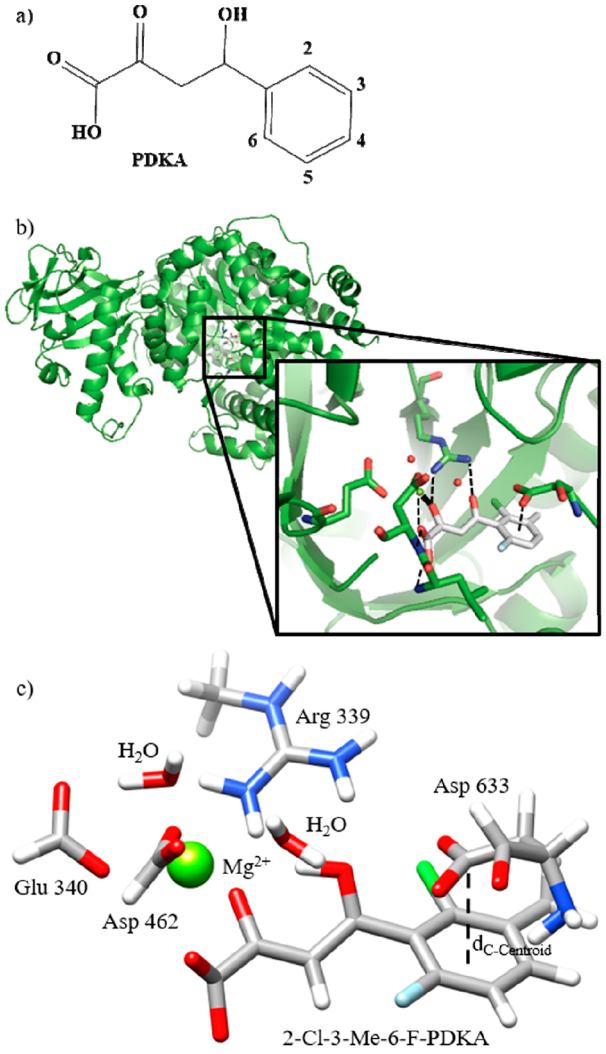

Figure 1. PDKA and PDKA-GlcB information: a) PDKA framework with labeled phenyl positions 2−6; b) Crystal structure of GlcB bound to 2-F-3-Me-6-Cl-PDKA (PDB: 3SB0).[10] (Inset) GlcB active site and the residues that participate in close-contacts (green framework) with the PDKA (white framework). Supramolecular interactions identified by dashed lines; c) PDKA-GlcB model active site, including four simplified residue analogues of Asp 633, Arg 339, Glu 340, and Asp 462; the catalytic Mg^{2+} ion; two water molecules and the monoanionic PDKA inhibitor.

PDKA due to the increase in the strength of the long-range anion-π interaction.[24] The calculations, however, fail to incorporate the steric constraints of the protein active site pocket in the calculations, which casts doubt on the validity of the predicted structures and interactions (Table S1 and Figure S1). Furthermore, the inconsistency of these predictions with the experimental structure−activity relationship (SAR) data belies the complexity of the biological and chemical contributions to inhibition and demonstrates the need for a more accurate computational model that appropriately accounts for the structural constraints of the full system. In this vein we have designed a computational active site (Figure 1c) that maintains biological integrity and allows for a more robust evaluation of the subtle interactions involved in the binding of PDKAs to GlcB.

In this study, we demonstrate that the PDKA-GlcB interaction can be suitably modeled using Density Functional

DOI: 10.1021/acs.jcim.8b00417
J. Chem. Inf. Model. 2018, 58, 2085−2091

Table 1. Library of PDKA Molecules Synthesized and Characterized in Complex with GlcB[a]

substituent(s) per PDKA	IC_{50} (μM)	PDB ID
2-Cl-3-Me-6-F (**1**)	5.5	3SB0
unsubstituted (**2**)	2.1	3S9I
2-F (**3**)	0.2	6C8P
2-Cl (**4**)	0.5	
2-Br (**5**)	0.6	3S9Z
2-Me	1.1	3SAD
2-Nitro	2.8	6DLJ
2,6-F	1.6	6DKO
2-F-3-Me-6-F	6.6	6DNP
2,6-Cl	1.0	6DL9
2-Cl-4-OH	0.007	6BA7
2-Br-3-OH	0.06	6BU1
2-Br-4-OH	0.005	6C6O
2-Br-6-Me	17.4	6C2X
3-OH	0.15	6APZ
3-Br	0.8	3SAZ
3-Prop-6-Me	15.2	6AS6
4-Me	6.1	6ASU
Per-F	>50	
dioxine	1.1	6AU9
naphthyl	0.5	6AXB
methoxynaphthyl	1.5	6C7B

[a]IC_{50} values for **1**−**5**, 2-Me-PDKA, 3-Me-PDKA, and 4-Me-PDKA previously reported by Krieger et al[10].

Theory (DFT) methods and that these calculations explain both the geometry of the interaction (as observed in crystal structures of complexes) as well as the enthalpies for analogs in this series. By appropriately conducting semiempirical quantum calculations with the necessary steric constraints and electronic contributions to the GlcB active site model, this study presents the first structure-based computational method that is capable of deriving PDKA-GlcB interaction energies that reproduce the SAR data with high correlation and, furthermore, is suitable for future evaluation of substituents for future predictions of improved PDKA inhibitors. These results are an effective validation of DFT methods and support the conclusion that the driving forces in this system are ultimately electrostatic in nature. These methods provide a medicinal chemistry guide for the future of structure-based drug design in systems involving weak, noncovalent interactions, in particular the anion-π interaction.

EXPERIMENTAL DETAILS

Protein Crystal Structures. *Mtb* malate synthase was overexpressed in *E. coli*, purified, and crystallized as described in previous studies by Krieger et al.[10] All PDKA ligands at the final concentration 0.5−5 mM were soaked overnight into preformed malate synthase crystals. After cryo-protecting with Fomblin HVAC (Sigma), crystals were flash-frozen for the data collection. Data were collected on the rotating anode home source instruments (RAXIS and BRUKER), as well as at the APS synchrotron 19 and 23ID beamlines of the Argonne National Lab. Diffraction data were indexed, integrated, and scaled in HKL2000.[25] Data were truncated in CCP4.[26] Model 1N8I of the isomorphous $P4_32_12$ crystal with only the protein atoms included in the refinement was used for the initial rigid body refinement in REFMAC.[27] Then, iterative runs of inspection and manual modification in COOT[28] and refinement in PHENIX[29] with simulated annealing were done to gradually improve the model. The ligand model and dictionary files were created in ELBOW BUILDER from the PHENIX suite and fitted into the density in COOT. For data collection and refinement statistics see Table S2. For **3**, **5**, 2-Me-PDKA, 2-F-2-Me-PDKA, and 2-Br-3-OH-PDKA, multiple conformations were built for portions of the active site. The atomic coordinates of the residue orientations with highest occupancy were retained for the model active site analysis. For 3-OH-PDKA, two alternative conformations were modeled for the ligand, which we denoted as 3-OH-PDKA (refined to 0.17 occupancy) and 5-OH-PDKA (refined to 0.83 occupancy).

Protein Inhibition Studies. IC_{50} values were determined by testing serial dilution of PDKA inhibitors in 5,5′-dithiobis(2-nitrobenzoic acid) (DTNB) coupled assay of malate synthase enzymatic activity as described in previous studies by Krieger et al.[10] Each data point for the IC_{50} plots was measured in duplicate.

Isothermal Calorimetry (ITC). ITC measurements were performed using MicroCal iTC_{200} instrument by titrating PDKA ligand into 50 μM solution of malate synthase equilibrated at 25 °C. Both the enzyme and the ligand were dissolved in the same enzyme activity assay buffer (20 mM TRIS-HCl pH = 7.5, 5 mM $MgCl_2$ 0.8 mM EDTA) with 1% DMSO.

Computational Methods. All GlcB model active sites, PDKA substrates, PDKA analogues, and chloride anions were partially- or fully optimized, as described in the text, using the M06-2X density functional theory functional[30] and the 6-31+G(d) basis set in Gaussian 09.[31] Each calculation was performed using a fine DFT integration grid to account for the sensitivity of the M06-2X functional to integration grid density.[32] This functional has been shown to appropriately evaluate weak, noncovalent interactions, such as anion-π interactions,[23,33] and is recommended for modeling noncovalent interactions in biological systems.[34] Interaction energies were obtained from the partially optimized and fully optimized calculations, as appropriate, as a difference in energy between the final complex and the sum of the parts.

RESULTS AND DISCUSSION

A simplified, biologically relevant model active site (Figure 1c) was developed through comparative analysis of 20 PDKA-bound GlcB crystal structures (Table 1, Figure S2, Table S2). In the model active site, the PDKA ligand is deprotonated at the terminal carboxylate group and occupies an overall charge-neutral binding pocket. The PDKA binds as a ditopic ligand to the catalytic magnesium ion. The octahedral coordination environment of the catalytic Mg^{2+} includes Glu 340 and Asp 462 (simplified to formate anions) and two water molecules. The approximate Mg^{2+} coordination environment is retained to provide the appropriate electrostatic interaction between each PDKA and the Mg^{2+} ion. The Arg 339 residue is simplified to amino(methylamino)methaniminium and is included in the active site model. This positively charged residue fragment participates in hydrogen-bonding interactions with the PDKA along the diketo acid tail, balances the charge of the active site, and provides steric and electrostatic contributions to the orientation of Asp 633. The final component of the active site is the Asp 633 residue which is deprotonated at the terminal carboxylate. Asp 633 participates in long-range electrostatic interactions with Mg^{2+} and Arg 339

DOI: 10.1021/acs.jcim.8b00417
J. Chem. Inf. Model. 2018, 58, 2085−2091

and in an anion-π interaction with the aryl portion of the PDKA inhibitor.

The PDKA-bound GlcB active site for 2-Cl-3-Me-6-F-PDKA (**1** bound to GlcB in PDB: 3SB0) was selected as the structural template for the construction of a predictive model. This active site template was chosen because **1** has demonstrated suitable activity against GlcB, and the electronegative substituents on **1** facilitate an archetypal, close anion-π interaction with Asp 633. Furthermore, of the templates investigated for this study (including templates based on **1**, **2**, 2-Nitro, 2-Cl-4-OH, 5-OH, dioxine, naphthyl-PDKA-GlcB structures), the active site of **1** most suitably reproduced the broad range of PDKA-GlcB interactions identified.

For each predictive model active site, the PDKA substituents in the template structure were modified in order to simulate each of the 22 unique PDKA compounds. The aforementioned comparative analysis of the PDKA-GlcB crystal structures indicated that the orientation of the entire active site is relatively fixed except for the positioning of the Asp 633 residue (Figure S2). The configuration of the Asp 633 residue therefore is a sensitive characteristic of the binding interactions of each PDKA in the active site. Informed by this structural analysis, each model active site was partially optimized using the M06-2X density functional theory (DFT) functional[30] and the 6-31+G(d) basis set in Gaussian 09.[31] In each calculation, the atomic coordinates of the heteroatoms that anchor the backbone of Asp 633 and the non-hydrogen atoms comprising the PDKA inhibitor (except for the substituents), Mg^{2+}, water molecules, Asp 462, Glu 340, and Arg 339 were constrained (gray atoms in Figure 2a). The remaining atoms of Asp 633, the hydrogen atoms, and the modified aryl substituents were optimized (green atoms in Figure 2a).

Upon partial-optimization of each of the predictive model active sites, the distance between the carbon atom of the Asp 633 carboxylate group and the centroid of the PDKA aryl moiety was measured ($d_{\text{C-Centroid}}$ as denoted by the dashed line in Figure 2a) and compared to the $d_{\text{C-Centroid}}$ of each respective crystal structure (see Figure 2b, Table S3). The average $d_{\text{C-Centroid}}$ accuracy across the entire predictive model series is 0.16 Å, well within the precision of atom locations for this crystallographic data (0.2 Å average across the data sets, as estimated from Luzzati plots).

The active site template facilitates highly accurate $d_{\text{C-Centroid}}$ calculations for PDKAs with more electronegative substituents, accurate to within 0.02 and 0.04 Å for 2-F-PDKA (**3**) and 2-Br-PDKA (**5**) respectively. For PDKAs with less electronegative substituents and for PDKA-GlcB crystal structures that exhibit $d_{\text{C-Centroid}}$ values greater than 3.7 Å, $d_{\text{C-Centroid}}$ calculations are less accurate due to the active site template being predisposed for close PDKA-Asp 633 contact (based on the relatively short anion-π contact in the **1**-GlcB template). For example, the calculation of the $d_{\text{C-Centroid}}$ distance for the GlcB complex with **2** is only accurate to within 0.24 Å, but this prediction is still within the precision of the crystal data as determined by Luzzati plots. Select overlays of the respective crystal structure and predictive model active sites for **2**, **3**, and **5** visually demonstrate the ability of the predictive model to reproduce the orientation of Asp 633 relative to the PDKA phenyl ring in the active site, Figure 2c.

While the predictive model accurately reproduces the geometry of the Asp 633-PDKA interaction, the computational assessment must also predict the relative binding strength of each PDKA-GlcB complex in order to be compelling for use in guiding drug development. To evaluate the predictive model's electronic treatment of the active site, the PDKA-GlcB binding enthalpies were calculated for each of the 22 predictive model active sites. Each binding enthalpy was determined as the energetic difference between the PDKA-GlcB complex and the sum of the uncomplexed substrate and active site.

There does not exist an obvious pattern between the PDKA substituents, PDKA-GlcB interaction energies, and the expanded library of SAR data, see Table 1. Generally, PDKAs with bulky substituent groups or multiple strongly

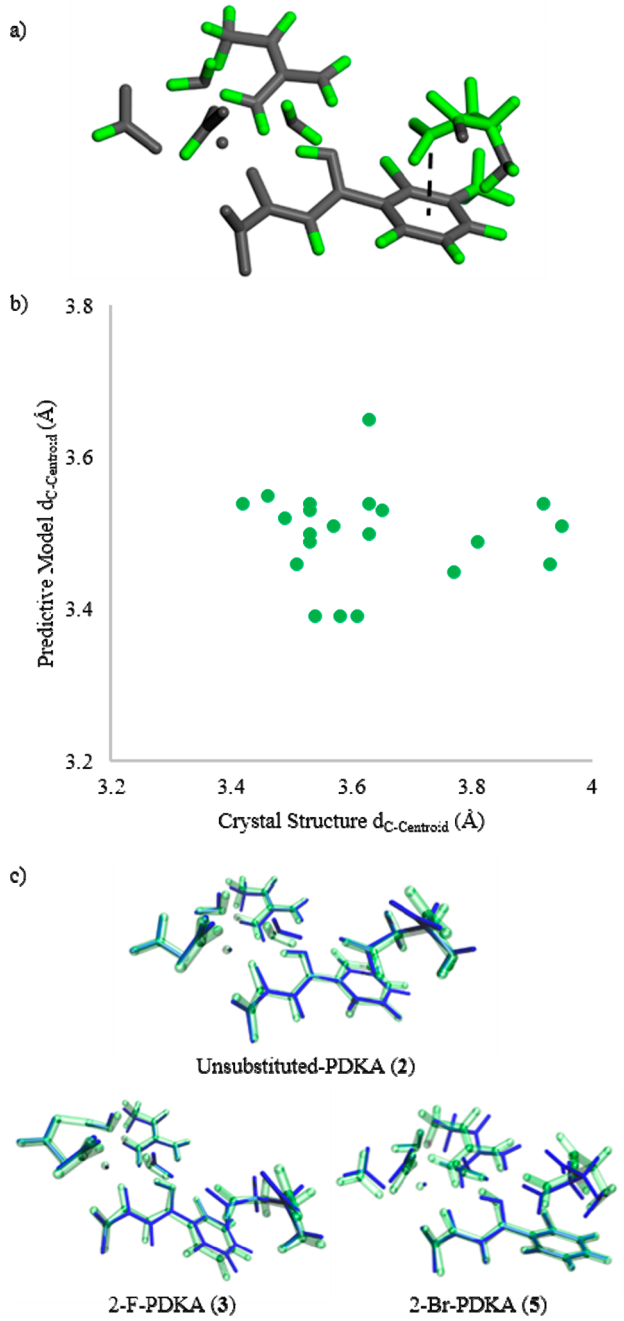

Figure 2. Predictive model of PDKA-GlcB binding: a) Predictive model 1-GlcB with the optimized atoms identified in green. $d_{\text{C-Centroid}}$ denoted by dashed line; b) Comparison of the $d_{\text{C-Centroid}}$ values of the predictive model with each respective crystal structure; c) Overlays of the respective crystal structure (blue with optimized hydrogen atom orientation) and partially optimized predictive model active sites (green) for **2**, **3**, and **5**.

DOI: 10.1021/acs.jcim.8b00417
J. Chem. Inf. Model. 2018, 58, 2085−2091

electronegative substituents result in high IC_{50} values, while the lowest IC_{50} values are exhibited by PDKAs with only one or two electronegative substituents at the 2 and 6 positions and one hydroxyl or methyl group at the 3 or 4 position. Therefore, to simplify the myriad factors that influence PDKA inhibitory activity and to isolate the influence of substituent choice on PDKA binding in the active site, isothermal calorimetry (ITC) studies were performed on **2** and the 2-*ortho halide*-PDKA compounds (**3**, 2-Cl-PDKA (**4**), and **5**) in complex with GlcB. This series of PDKA-GlcB complexes was selected in order to deconvolute the impact of the anion-π interaction on binding affinity from the steric and electronic effects of additional substituents at other positions. The predictive model binding enthalpies of **2**−**5** (relative to the ITC enthalpy for **2**) were compared to the corresponding ITC data, specifically the binding enthalpy, Figure 3a. The correlation between the predictive model and experimental binding enthalpies suggests that the predictive model template appropriately captures the steric and electronic factors that influence the 2-*ortho halide*-PDKA-GlcB binding enthalpies. As shown by both the experimental and computational studies, the magnitude of the interaction energy increases as the size of the PDKA substituent increases. This is consistent with results for model anion-π interactions previously described by Wheeler and co-workers.[33] The slight deviation from an ideal linear regression may be a result of small steric or long-range electrostatic factors in the intact protein that are not accounted for in the predictive model. Contributions to PDKA-GlcB binding from other residues in the active site or greater protein structure that are not included in this model are inconsequential for the purpose of comparing the binding of the ligands within a set of close analogs. It also underscores the conclusion that anion-π interactions drive the difference in the inhibitory activity within the series.

In accordance with our initial objectives, the template-based predictive model appropriately describes the steric (the Asp 633-PDKA orientation upon binding) and electronic environment (the relative 2-*ortho halide*-PDKA binding enthalpies) of the PDKA-bound GlcB active site. Unfortunately, partial-optimization of each predictive model active site is prohibitively time-intensive for use as a comprehensive screening tool for new PDKA drug development. In order to more efficiently explore the binding enthalpies of new PDKA derivatives, a simplified screening model was developed as a way to narrow the field of promising small-molecule candidates for further analysis by the predictive model. The initial comparative analysis identified that the primary structural difference across the series of PDKA-GlcB complexes is the anion-π interaction between the flexible Asp 633 side chain and each PDKA, so the screening model focused on this difference. Analogously substituted benzene rings were used to model each of the PDKAs, and a chloride ion was used to approximate the Asp 633 side chain carboxylate. Chloride was selected because it is a symmetrically simple, computationally affordable anion that streamlines the evaluation of the anion-π interaction, and because chloride has previously been used in anion-substituted benzene model systems to study anion-π interactions and substituent effects.[23,34,35] In each screening model complex, the chloride was located directly above the centroid of each of the fully optimized aromatic molecules, the atoms of the benzene molecules were restrained, and the Cl^- was optimized along the *z*-axis at the M06-2X/6-31+G(d) level of theory (see inset of Figure 3b). The anion-π interaction

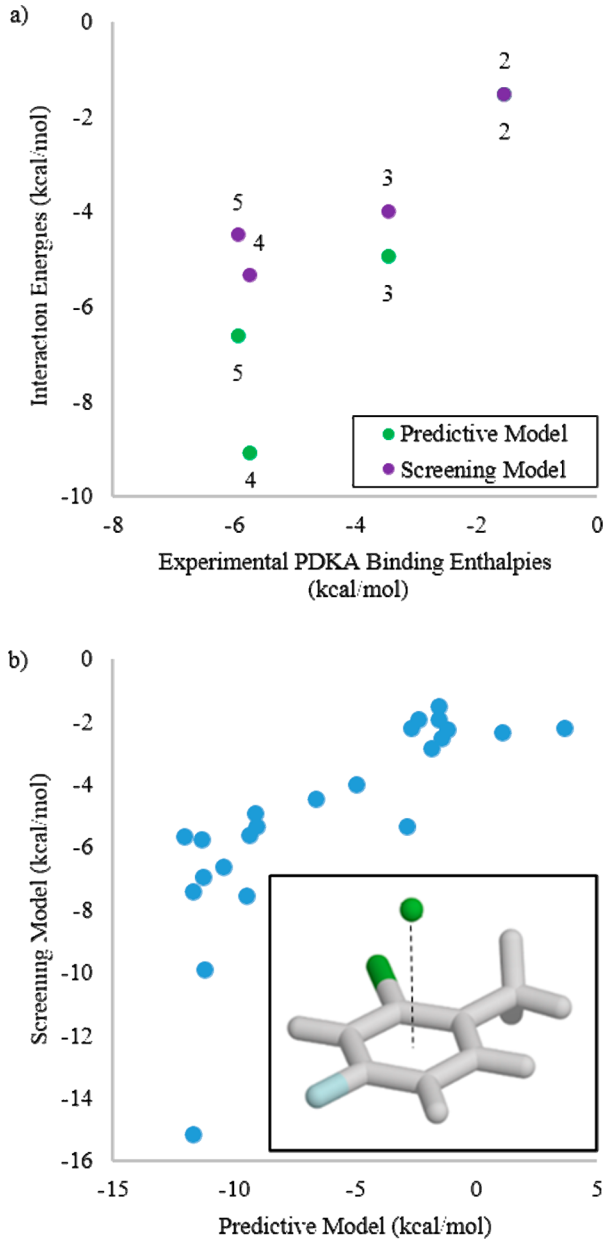

Figure 3. Comparison of the screening model, predictive model, and experimental data. a) Comparison of the PDKA binding enthalpies of the ITC experiments with the predictive model interaction energies (green series) and the screening model (purple series), where the predictive and screening models are relative to the ITC enthalpy for **2**; b) Correlation between the interaction energies in the screening and predictive models (predictive model data shown relative to ITC enthalpy for **2**). (Inset) Substituted-benzene analogue of **1** in complex with Cl^-. The complex was partially optimized along the Cl^--centroid axis, denoted by the dashed line.

energies were calculated for each of the resulting screening model complexes and are in agreement with previous studies regarding substituent effects on anion-π interactions.[23,34,35]

A high correlation exists between the anion-π interaction energies predicted by the screening model (relative to the ITC-based enthalpy for **2**) and the ITC-derived binding enthalpies for the 2-*ortho halide*-PDKA series, Figure 3a. The difference between the screening model interaction energies and the ITC binding enthalpies results from the additional noncovalent interactions that participate in binding in the biological active

DOI: 10.1021/acs.jcim.8b00417
J. Chem. Inf. Model. 2018, 58, 2085−2091

site, but the correlation of the experimental and theoretical data suggests that these additional binding interactions are relatively constant for **2**−**5**. Therefore, while the anion-π interaction may not be the strongest interaction in the active site, it is the factor that determines fine control over the binding enthalpy of PDKA-GlcB.

Furthermore, the relative interaction energies from both the predictive and screening models are correlated across the entire series of PDKAs (see Figure 3b and Table S3). Variations in the anion-π interaction probed by the screening model for each PDKA analogue captures the trend in the overall interaction energy, as calculated by the more comprehensive predictive model. The screening model describes the substituent effects on each respective anion-π interaction, but the predictive model is needed to more carefully evaluate the fine impact of varying the substituent position on the PDKA phenyl ring, especially the effect on the other interactions of the PDKA in the active site as permitted by the constraints of the GlcB active site framework.

While the screening model does not incorporate the structural constraints associated with the GlcB active site, this simplified model can be used as a computationally efficient method to evaluate the relative affinity of PDKAs that favorably bind in the model active site. Future efforts will employ the screening model to narrow the field of PDKA candidates to those that will facilitate favorable anion-π interactions and increased binding enthalpies. The predictive model can then be applied to this pared-down list of candidates in order to more thoroughly interrogate the additional interactions involved for each PDKA and how they are expected to influence the PDKA-GlcB binding.

CONCLUSIONS

While anion-π interactions are being increasingly identified for their importance in biological systems, these noncovalent forces have yet to be incorporated into modern structure-based CADD methodologies. Further motivated by the continued need for advancements in TB treatments, we have demonstrated the importance of including anion-π interactions in CADD assessments of biological systems, specifically the inhibition of GlcB by PDKAs.

An active site template was developed for our predictive model by incorporating key components of the active site from the **1**-GlcB crystal structure that facilitated appropriate electrostatic, hydrogen-bonding, and anion-π interactions and maintained structural integrity of the active site. A predictive model has been developed and shown to accurately replicate the orientation of the Asp 633 residue as it interacts with each of the PDKAs, with an average $d_{\text{C-Centroid}}$ accuracy of 0.16 Å. In addition to functioning as a suitable steric model, the predictive model appropriately handles the cooperativity and substituent effects of the noncovalent interactions that influence PDKA binding in the active site. The PDKA-GlcB interaction energies for the 2-*ortho halide*-PDKA series calculated by the predictive model are correlated with the experimental binding enthalpies determined by ITC. The predictive model is consistent with experimental data—simultaneously describing key PDKA-GlcB architectural factors and modeling PDKA binding enthalpies.

To improve the computational efficiency of the predictive model, we have also developed a screening model that determines the propensity of each PDKA to participate in anion-π interactions. The series of anion-π interaction energies of the PDKA analogues was shown to be directly proportional to the interaction energies of the predictive model and the experimental ITC binding enthalpies. The screening model highlights the fine control over PDKA-binding that is governed by the anion-π interaction and provides a simple tool for preliminary screening of potential PDKA analogue candidates for synthesis.

Future studies will couple the screening and predictive models to evaluate favorable PDKA ligands and identify the most ideal PDKA candidates for further experimental studies. Through this study, we have demonstrated the importance of appropriately incorporating anion-π interactions into CADD methodologies, thereby providing a guide for future medicinal chemistry pursuits.

ASSOCIATED CONTENT

Supporting Information

The Supporting Information is available free of charge on the ACS Publications website at DOI: 10.1021/acs.jcim.8b00417.

Further evaluation of the level of theory and system, crystal data and refinement information, comparative analysis of active sites, computational model template coordinates, and additional computational data (PDF)
Excel file (XLSX)

Accession Codes

Authors will release the atomic coordinates and experimental data upon article publication (PDKA-bound GlcB, PDB ID): 2-F (**3**), 6C8P; 2-Nitro, 6DLJ; 2,6-F, 6DKO; 2-F-3-Me-6-F, 6DNP; 2,6-Cl, 6DL9; 2-Cl-4-OH, 6BA7; 2-Br-3-OH, 6BU1; 2-Br-4-OH, 6C6O; 2-Br-6-Me, 6C2X; 3-OH, 6APZ; 3-Prop-6-Me, 6AS6; 4-Me, 6ASU; dioxine, 6AU9; naphthyl, 6AXB; methoxynaphthyl, 6C7B.

AUTHOR INFORMATION

Corresponding Author

*E-mail: dunbar@chem.tamu.edu.

ORCID

Jill F. Ellenbarger: 0000-0001-8809-3843
James C. Sacchettini: 0000-0001-5767-2367
Steven E. Wheeler: 0000-0001-7824-6906
Kim R. Dunbar: 0000-0001-5728-7805

Notes

The authors declare no competing financial interest.

ACKNOWLEDGMENTS

We would like to thank the Texas A&M University Supercomputing Center and Dr. Lisa Pérez in the Laboratory of Molecular Simulation for providing computational resources and support. K.R.D. gratefully acknowledges the generous support from the National Science Foundation for Grant CHE-1310574. J.C.S. gratefully acknowledges the generous support from the National Institute of Allergy and Infectious Diseases of the National Institutes of Health for the TB Structural Genomics grant P01A1095208 and from the Welch foundation for Grant A-0015.

REFERENCES

(1) Global Tuberculosis Report 2017; World Health Organization: Tuberculosis Publications Web Site, 2017. http://www.who.int/tb/publications/global_report/en/ (accessed Feb 6, 2018).

DOI: 10.1021/acs.jcim.8b00417
J. Chem. Inf. Model. 2018, 58, 2085−2091

(2) Smith, C. V.; Sharma, V.; Sacchettini, J. C. TB Drug Discovery: Addressing Issues of Persistence and Resistance. *Tuberculosis* **2004**, *84*, 45−55.
(3) Sacchettini, J. C.; Rubin, E. J.; Freundlich, J. S. Drugs Versus Bugs: In Pursuit of the Persistent Predator Mycobacterium Tuberculosis. *Nat. Rev. Microbiol.* **2008**, *6*, 41−52.
(4) Sliwoski, G.; Kothiwale, S.; Meiler, J.; Lowe, E. W. Computational Methods in Drug Discovery. *Pharmacol. Rev.* **2014**, *66*, 334−395.
(5) Ban, F.; Dalal, K.; Li, H.; LeBlanc, E.; Rennie, P. S.; Cherkasov, A. Best Practices of Computer-Aided Drug Discovery: Lessons Learned from the Development of a Preclinical Candidate for Prostate Cancer with a New Mechanism of Action. *J. Chem. Inf. Model.* **2017**, *57*, 1018−1028.
(6) Mahadevi, A. S.; Sastry, G. N. Cation−π Interaction: Its Role and Relevance in Chemistry, Biology, and Material Science. *Chem. Rev.* **2013**, *113*, 2100−2138.
(7) Lucas, X.; Bauzá, A.; Frontera, A.; Quiñonero, D. A Thorough Anion-π Interaction Study in Biomolecules: On the Importance of Cooperativity Effects. *Chem. Sci.* **2016**, *7*, 1038−1050.
(8) Ioerger, T. R.; O'Malley, T.; Liao, R.; Guinn, K. M.; Hickey, M. J.; Mohaideen, N.; Murphy, K. C.; Boshoff, H. I. M.; Mizrahi, V.; Rubin, E. J.; Sassetti, C. M.; Barry, C. E.; Sherman, D. R.; Parish, T.; Sacchettini, J. C. Identification of New Drug Targets and Resistance Mechanisms in Mycobacterium Tuberculosis. *PLoS One* **2013**, *8*, e75245.
(9) Kana, B. D.; Karakousis, P. C.; Parish, T.; Dick, T. Future Target-Based Drug Discovery for Tuberculosis? *Tuberculosis* **2014**, *94*, 551−556.
(10) Krieger, I. V.; Freundlich, J. S.; Gawandi, V. B.; Roberts, J. P.; Gawandi, V. B.; Sun, Q.; Owen, J. L.; Fraile, M. T.; Huss, S. I.; Lavandera, J. L.; Ioerger, T. R.; Sacchettini, J. C. Structure-Guided Discovery of Phenyl-Diketo Acids as Potent Inhibitors of M. Tuberculosis Malate Synthase. *Chem. Biol.* **2012**, *19*, 1556−1567.
(11) Payne, D. J.; Gwynn, M. N.; Holmes, D. J.; Pompliano, D. L. Drugs for Bad Bugs: Confronting the Challenges of Antibacterial Discovery. *Nat. Rev. Drug Discovery* **2007**, *6*, 29−40.
(12) McKinney, J. D.; Höner zu Bentrup, K.; Munoz-Elias, E. J.; Miczak, A.; Chen, B.; Chan, W. T.; Swenson, D.; Sacchettini, J. C.; Jacobs, W. R.; Russell, D. G. Persistence of Mycobacterium Tuberculosis in Macrophages and Mice Requires the Glyoxylate Shunt Enzyme Isocitrate Lyase. *Nature* **2000**, *406*, 735−738.
(13) Munoz-Elias, E. J.; McKinney, J. D. Mycobacterium Tuberculosis Isocitrate Lyases 1 and 2 are Jointly Required for In Vivo Growth and Virulence. *Nat. Med.* **2005**, *11*, 638−644.
(14) Anstrom, D. M.; Remington, S. J. The Product Complex of M-Tuberculosis Malate Synthase Revisited. *Protein Sci.* **2006**, *15*, 2002−2007.
(15) Smith, C. V.; Huang, C. C.; Miczak, A.; Russell, D. G.; Sacchettini, J. C.; Höner zu Bentrup, K. Biochemical and Structural Studies of Malate Synthase from Mycobacterium Tuberculosis. *J. Biol. Chem.* **2003**, *278*, 1735−1743.
(16) Schottel, B. L.; Chifotides, H. T.; Dunbar, K. R. Anion-π Interactions. *Chem. Soc. Rev.* **2008**, *37*, 68−83.
(17) Alkorta, I.; Rozas, I.; Elguero, J. Interaction of Anions with Perfluoro Aromatic Compounds. *J. Am. Chem. Soc.* **2002**, *124*, 8593−8598.
(18) Mascal, M.; Armstrong, A.; Bartberger, M. D. Anion-Aromatic Bonding: A Case for Anion Recognition by π-Acidic Rings. *J. Am. Chem. Soc.* **2002**, *124*, 6274−6276.
(19) Quiñonero, D.; Garau, C.; Frontera, A.; Ballester, P.; Costa, A.; Deyà, P. M. Counterintuitive Interaction of Anions with Benzene Derivatives. *Chem. Phys. Lett.* **2002**, *359*, 486−492.
(20) Ribić, V. R.; Stojanović, S. Đ.; Zlatović, M. V. Anion−π Interactions in Active Centers of Superoxide Dismutases. *Int. J. Biol. Macromol.* **2018**, *106*, 559−568.
(21) Wilson, K. A.; Wetmore, S. D. Combining Crystallographic and Quantum Chemical Data to Understand DNA-Protein π-Interactions in Nature. *Struct. Chem.* **2017**, *28*, 1487−1500.
(22) Dougherty, D. A. The Cation-π Interaction. *Acc. Chem. Res.* **2013**, *46*, 885−893.
(23) Wheeler, S. E. Understanding Substituent Effects in Noncovalent Interactions Involving Aromatic Rings. *Acc. Chem. Res.* **2013**, *46*, 1029−1038.
(24) Bauzá, A.; Quiñonero, D.; Deyà, P. M.; Frontera, A. Long-Range Effects in Anion-π Interactions: Their Crucial Role in the Inhibition Mechanism of Mycobacterium Tuberculosis Malate Synthase. *Chem. - Eur. J.* **2014**, *20*, 6985−6990.
(25) Otwinowski, Z.; Minor, W. [20] Processing of X-Ray Diffraction Data Collected in Oscillation Mode. *Methods Enzymol.* **1997**, *276*, 307−326.
(26) Potterton, E.; McNicholas, S.; Krissinel, E.; Cowtan, K.; Noble, M. The CCP4Molecular-Graphics Project. *Acta Crystallogr., Sect. D: Biol. Crystallogr.* **2002**, *58*, 1955−1957.
(27) Murshudov, G. N.; Skubak, P.; Lebedev, A. A.; Pannu, N. S.; Steiner, R. A.; Nicholls, R. A.; Winn, M. D.; Long, F.; Vagin, A. A. REFMAC5 for the Refinement of Macromolecular Crystal Structures. *Acta Crystallogr., Sect. D: Biol. Crystallogr.* **2011**, *67*, 355−367.
(28) Emsley, P.; Lohkamp, B.; Scott, W. G.; Cowtan, K. Features and Development of Coot. *Acta Crystallogr., Sect. D: Biol. Crystallogr.* **2010**, *66*, 486−501.
(29) Adams, P. D.; Grosse-Kunstleve, R. W.; Hung, L.-W.; Ioerger, T. R.; McCoy, A. J.; Moriarty, N. W.; Read, R. J.; Sacchettini, J. C.; Sauter, N. K.; Terwilliger, T. C. PHENIX: Building New Software for Automated Crystallographic Structure Determination. *Acta Crystallogr., Sect. D: Biol. Crystallogr.* **2002**, *58*, 1948−1954.
(30) Zhao, Y.; Truhlar, D. The M06 Suite of Density Functionals for Main Group Thermochemistry, Thermochemical Kinetics, Noncovalent Interactions, Excited States, and Transition Elements: Two New Functionals and Systematic Testing of Four M06-Class Functionals and 12 Other Functionals. *Theor. Chem. Acc.* **2008**, *120*, 215−241.
(31) Frisch, M. J.; Trucks, G. W.; Schlegel, H. B.; Scuseria, G. E.; Robb, M. A.; Cheeseman, J. R.; Scalmani, G.; Barone, V.; Mennucci, B.; Petersson, G. A.; Nakatsuji, H.; Caricato, M.; Li, X.; Hratchian, H. P.; Izmaylov, A. F.; Bloino, J.; Zheng, G.; Sonnenberg, J. L.; Hada, M.; Ehara, M.; Toyota, K.; Fukuda, R.; Hasegawa, J.; Ishida, M.; Nakajima, T.; Honda, Y.; Kitao, O.; Nakai, H.; Vreven, T.; Montgomery, J. A., Jr.; Peralta, J. E.; Ogliaro, F.; Bearpark, M. J.; Heyd, J.; Brothers, E. N.; Kudin, K. N.; Staroverov, V. N.; Kobayashi, R.; Normand, J.; Raghavachari, K.; Rendell, A. P.; Burant, J. C.; Iyengar, S. S.; Tomasi, J.; Cossi, M.; Rega, N.; Millam, N. J.; Klene, M.; Knox, J. E.; Cross, J. B.; Bakken, V.; Adamo, C.; Jaramillo, J.; Gomperts, R.; Stratmann, R. E.; Yazyev, O.; Austin, A. J.; Cammi, R.; Pomelli, C.; Ochterski, J. W.; Martin, R. L.; Morokuma, K.; Zakrzewski, V. G.; Voth, G. A.; Salvador, P.; Dannenberg, J. J.; Dapprich, S.; Daniels, A. D.; Farkas, Ö.; Foresman, J. B.; Ortiz, J. V.; Cioslowski, J.; Fox, D. J. *Gaussian 09*, Revision B.01; Gaussian, Inc.: Wallingford, CT, USA, 2009.
(32) Wheeler, S. E.; Houk, K. N. Integration Grid Errors for Meta-GGA-Predicted Reaction Energies: Origin of Grid Errors for the M06 Suite of Functionals. *J. Chem. Theory Comput.* **2010**, *6*, 395−404.
(33) Wheeler, S. E.; McNeil, A. J.; Müller, P.; Swager, T. M.; Houk, K. N. Probing Substituent Effects in Aryl−Aryl Interactions using Stereoselective Diels−Alder Cycloadditions. *J. Am. Chem. Soc.* **2010**, *132*, 3304−3311.
(34) Wheeler, S. E.; Houk, K. N. Are Anion/π Interactions Actually a Case of Simple Charge-Dipole Interaction? *J. Phys. Chem. A* **2010**, *114*, 8658−8664.
(35) Bagwill, C.; Anderson, C.; Sullivan, E.; Manohara, V.; Murthy, P.; Kirkpatrick, C. C.; Stalcup, A.; Lewis, M. Predicting the Strength of Anion−π Interactions of Substituted Benzenes: The Development of Anion−π Binding Substituent Constants. *J. Phys. Chem. A* **2016**, *120*, 9235−9243.

DOI: 10.1021/acs.jcim.8b00417
J. Chem. Inf. Model. 2018, 58, 2085−2091